

Binocular Contributions to Optic Flow Processing in the Fly Visual System

HOLGER G. KRAPP,¹ ROLAND HENGSTENBERG,² AND MARTIN EGELHAAF¹

¹*Lehrstuhl für Neurobiologie, Fakultät für Biologie, Universität Bielefeld, D-33501 Bielefeld;*
and ²*Max-Planck-Institut für Biologische Kybernetik, D-72076 Tübingen, Germany*

Received 22 February 2000; accepted in final form 24 October 2000

Krapp, Holger G., Roland Hengstenberg, and Martin Egelhaaf. Binocular contributions to optic flow processing in the fly visual system. *J Neurophysiol* 85: 724–734, 2001. Integrating binocular motion information tunes wide-field direction-selective neurons in the fly optic lobe to respond preferentially to specific optic flow fields. This is shown by measuring the local preferred directions (LPDs) and local motion sensitivities (LMSs) at many positions within the receptive fields of three types of anatomically identifiable lobula plate tangential neurons: the three horizontal system (HS) neurons, the two centrifugal horizontal (CH) neurons, and three heterolateral connecting elements. The latter impart to two of the HS and to both CH neurons a sensitivity to motion from the contralateral visual field. Thus in two HS neurons and both CH neurons, the response field comprises part of the ipsi- and contralateral visual hemispheres. The distributions of LPDs within the binocular response fields of each neuron show marked similarities to the optic flow fields created by particular types of self-movements of the fly. Based on the characteristic distributions of local preferred directions and motion sensitivities within the response fields, the functional role in the context of behaviorally relevant proc motion is discussed.

INTRODUCTION

Visual motion is due to relative movements between the eyes of an observer and the visual structures of the environment. The resulting motion pattern over the observer's eyes is commonly referred to as "optic flow" (Gibson 1950), which is a description of retinal image movements in terms of local velocity vectors. The global structure of optic flow fields reflects the observer's mode of self-motion, i.e., rotation, translation, or a combination of both (Koenderink and van Doorn 1987, reviews: Lappe 2000; Lappe et al. 1999). During translation, nearby objects induce larger flow vectors than more distant objects. Thus translation induced optic flow contains relative distance information about the three-dimensional environment.

In the nervous system, optic flow is initially analyzed by arrays of retinotopically arranged local direction-selective elements (review: e.g., Borst and Egelhaaf 1989). Local motion analysis on its own, however, does not allow the system to decide whether self-translation or -rotation induced the respective retinal image shift. A common strategy to disambiguate the situation is to spatially integrate motion information. The

specificity of such integrating elements to sense rotatory or translatory self-movement can be further enhanced if motion information from both visual hemispheres is combined. In vertebrates with laterally positioned eyes, such as rabbits and birds, as well as in arthropods equipped with panoramic vision, extensive spatial pooling of motion information and interactions between both eyes were shown to increase the sensitivity to particular optic flow fields (rabbits e.g., Leonard et al. 1988; birds e.g., Wylie and Frost 1999; crustaceans: Kern et al. 1993; Nalbach and Nalbach 1987; insects e.g., Hausen and Egelhaaf 1989; Ibbotson 1991; Kern 1998; Kern and Varjú 1998).

In the fly lobula plate, which is the final neuropile in the optic lobe, approximately 50–60 individually identifiable tangential neurons have been found (Hausen 1984). Tangential neurons receive ipsilateral visual input from many retinotopically arranged elementary movement detectors (EMDs) (reviewed by Hausen et al. 1993). This is leading to receptive field organization that matches the global structure of optic-flow fields induced by self-rotations around horizontally aligned body axes (Franz and Krapp 2000; Krapp 2000; Krapp and Hengstenberg 1996).

To what degree does binocular vision increase the specificity of tangential neurons to sense particular self-movements? To answer this question, we investigated the receptive field organization of the horizontal system (HS) and centrifugal horizontal (CH) wide-field tangential neurons (Dvorak et al. 1975; Hausen 1976b, 1982a,b), which are thought to be involved in optomotor course control (HS neurons) and figure-ground discrimination (CH neurons) (Hausen and Wehrhahn 1989; review: Egelhaaf and Borst 1993; Hausen and Egelhaaf 1989). Besides their ipsilateral retinotopic inputs, most of these neurons receive contralateral motion information (Egelhaaf et al. 1993; Hausen 1976a, 1981; Horstmann et al. 2000). Here we determine the local preferred directions (LPDs) and local motion sensitivities (LMSs) at many positions within the ipsi- and

Present address and address for reprint requests: H. G. Krapp, Dept. Zoology, Cambridge University, Downing Street, Cambridge CB2 3EJ, UK (E-mail: hgk23@hermes.cam.ac.uk).

The costs of publication of this article were defrayed in part by the payment of page charges. The article must therefore be hereby marked "advertisement" in accordance with 18 U.S.C. Section 1734 solely to indicate this fact.

contralateral visual hemispheres. Furthermore we present the receptive field organization of heterolateral connecting elements, which are thought to mediate the contralateral input to the binocular HS and CH neurons. Based on the HS and CH neurons' local response properties, it is quantitatively estimated how their monocular specificity to particular self-movements is influenced by their binocular input.

METHODS

Preparation

Experiments were performed with 1- to 2-day-old female blowflies of the genus *Calliphora*. Before dissection for electrophysiology, the animals were briefly anesthetized with CO₂. Legs and wings were removed and the head was tilted forward and fixed to a holder. Alignment with the visual stimulus device was achieved by adjusting the head according to the symmetrical deep pseudopupil (Franceschini 1975) in the frontal region of both eyes. For intracellular recordings, the gut and muscles of the mouth parts were removed to reduce brain movements. After opening the head capsule from behind to get access to the lobula plate, fat tissue, air sacs, and tracheae were removed. Wounds, except the opening in the head capsule, were closed with wax to prevent the animal from desiccation. By adding saline solution, the nervous tissue was kept moist (Hausen 1982a).

Electrophysiology

Extracellular tungsten electrodes with an impedance of about 2 M Ω were used to record action potentials from the heterolateral connecting elements H1, H2, and V1. For intracellular recording, we pulled glass capillaries (Clark, GC 100F-10) on a Brown Flammig puller (Sutter Instruments, P87). The tips were either filled with a solution of 3% Lucifer yellow CH (Sigma) in 1 M LiCl, and the shaft with 1 M LiCl or the entire electrode was filled with 1 M KCl. The resistance of the electrodes was 40–60 M Ω . In all recordings, a tip-broken glass capillary was used as a ground electrode and to supply the brain with saline solution. We used electrophysiological standard equipment for the recordings (see Krapp et al. 1998). Extracellularly recorded spikes were converted into unit-pulses and sampled at a rate of 0.72 kHz. Intracellularly recorded signals were sampled at the same rate. Programs for data acquisition and evaluation, as well as for controlling visual stimulation, were written in ASYST 4.0 (Macmillan Software).

Identification of investigated neurons

Most of the intracellularly recorded neurons were injected with Lucifer yellow and identified *in situ* immediately after the experiments by fluorescence microscopy (Zeiss, Axiophot, fluorescein isothiocyanate filter combination). Due to their anatomical characteristic, the HS neurons could be easily distinguished from each other as well as from the two CH neurons (Hausen 1981). The response fields of individual tangential neurons are remarkably reproducible from animal to animal and can thus be considered a characteristic fingerprint (Krapp et al. 1998). Therefore in later experiments, Lucifer yellow was no longer applied, and the identification was achieved according to the response fields.

The heterolateral H1 neuron can be identified unambiguously by recording from its output region in the left lobula plate and stimulating the contralateral eye from which it receives its input (Hausen 1976b). H2, like H1, is sensitive to horizontal back-to-front motion over the right eye and conveys its spikes to the contralateral part of the brain. The H2 recording reported here took place within its dendritic input region. H2 was distinguished from H1 by means of physiological differences between the neurons. First, the spontaneous activity of H2 is almost zero, whereas H1 spontaneously generates spikes at rates between 10 and 40 Hz. Second, the maximum firing rate of H2 is much lower compared with H1 firing rates (Warzecha et al. 1998). Third, the sensitivity distribution within the response field of H1 is much broader than that of H2 (cf. Fig. 4, A and B). The V1 spikes were recorded within the neuron's output ramifications contralateral to the side of its input region in the ventrolateral protocerebrum. V1 is as yet the only known spiking heterolateral element that is sensitive to vertical downward motion in the frontal to frontolateral visual field (Hausen 1976b; Krapp and Hengstenberg 1997).

Determining the local response properties

The LPDs and LMSs were determined according to a procedure that was described in detail by Krapp and Hengstenberg (1997). A black dot ($\varnothing = 7.6^\circ$) is moved along a circular path ($\varnothing = 10.4^\circ$) at 2 cycles/s for several cycles in a clockwise (cw) and subsequently in a counterclockwise (ccw) direction (Fig. 1A). During intracellular recordings, three cycles in each direction were enough to reliably determine the LPD (Fig. 1B); during extracellular recordings, 10 cycles per direction were presented. When the instantaneous direction of dot motion and the preferred direction of the small field elements converging on the recorded neuron coincide, the measured response becomes maximum. An unknown phase-shift caused by response delays can be estimated and corrected by comparing the responses to

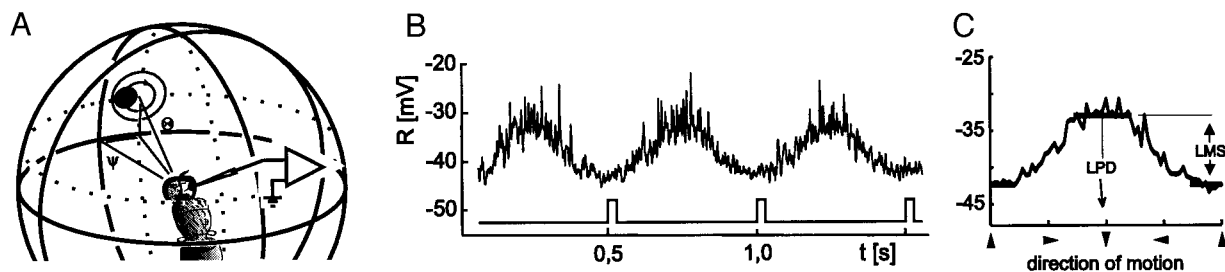


FIG. 1. Determining the local response properties of direction-selective wide-field neurons. A: the stimulus consists of a black dot (7.6° diam) moving at constant speed (2 cycles/s) along a circular path (10.4° diam). The stimulus position is defined by its azimuth φ and elevation θ . For example, during dot motion in a clockwise direction (cw), responses of tangential neurons are recorded either intra- or extracellularly. B: consecutive motion cycles result in a periodic change of the neuronal activity (here: membrane potential). Within each cycle, the maximum response is reached when the momentary direction of dot motion coincides with the recorded neuron's local preferred direction (LPD). Unit pulses elicited once per cycle allow us to reconstruct the momentary direction of dot motion (see *bottom trace*). C: the phase-locked average of 3–10 response traces obtained from the respective number of stimulus cycles is further pooled into 72 bins, each containing the mean response to 5° intervals representing different motion directions. After correcting for a delay-induced phase-shift, the LPD is determined by circular statistics. The local motion sensitivity (LMS) is the difference between the mean within a 90° -wide response interval centered on the LPD and the mean within a 90° -wide interval centered at LPD + 180° (thick horizontal bars). Details in Krapp and Hengstenberg (1997).

cw and ccw motion (Krapp and Hengstenberg 1997). The phase-locked average of the responses to cw and ccw motion, respectively, were pooled in 5° bins of successive dot motion directions (Fig. 1C). The mean LPD was determined by calculating the direction of the mean vector of the resulting circular response histogram (Batschelet 1981). To keep from losing information about the neurons' absolute response range induced by our local stimulus, we used a linear measure to define the LMS. It is defined as the difference between the response averaged within the interval of $\pm 45^\circ$ centered on the LPD and the response within an equally sized interval obtained during motion in the opposite direction (Fig. 1C).

Mapping the local response properties

In this report, we present results derived from different sets of experiments. Data gathered from the neurons H1 and H2 were obtained in animals whose left eye was occluded with nontoxic black acrylic paint to avoid binocular cross-talk. In these experiments, local motion stimuli were presented at 54 positions in the right visual hemisphere. In experiments that aimed to investigate the binocular input to HS and CH neurons and to V1, the number of measuring positions was 46 in the right and 30 positions in the left visual hemisphere. LPDs and LMSs are plotted as arrows in a Mercator map of the visual space where positions are defined by two angles: the azimuth φ and the elevation θ . Positive values of φ indicate positions in the right visual hemisphere. Positive values of θ denote positions above the eye equator. The orientation of each arrow gives the LPD and its length denotes the LMS, normalized to the respective maximum response of the recorded neuron. In the following, such maps of the neurons' local response properties are referred to as "response fields." The Mercator map inherently distorts the dorsal and the ventral part of the spherical visual field by the factor $1/\cos \theta$. To mediate a better impression of the global appearance of the response fields, we interpolated values between the actually measured data by applying a Matlab routine (Vers. 5.3). The LPDs measured at the given positions (φ , θ) were decomposed into their x and y components. This resulted—together with the respective LMS distribution—in three two-dimensional scalar fields. The interpolation algorithm used fits a smooth surface through two-dimensional scalar fields and is based on Delaunay-Triangulation (Watson 1994). The interpolated arrows in the response fields were then reconstructed from the interpolated x and y components, scaled by the interpolated LMSs. Within the response fields shown in RESULTS, all measured data are plotted in black; interpolated values are shown in gray.

In most of our experiments, we did not carry out the time-consuming histology and reconstruction but identified the stained neurons in situ. To nevertheless show the morphology of the investigated neurons, in the *insets* of Figs. 2–4, reconstructions are shown that were prepared, and kindly provided, by Hausen during his earlier studies (Hausen 1981, 1982a, 1993).

RESULTS

HS neurons

The horizontal system (HS) consists of three neurons: the HSN, HSE, and HSS (N, north; E, equatorial; S, south) (Hausen 1982a). Since HSS integrates only monocular motion information, data obtained from this neuron are not included in our present report. HSN dendrites occupy the dorsal part of the neuropil, whereas HSE dendrites ramify in the medial part of the lobula plate (Hausen 1982a) (cf. Fig. 2, *inset*). Horizontal front-to-back wide-field motion within the ipsilateral visual hemispheres leads in HSN and HSE to depolarizing membrane potential changes (Hausen 1982b). These graded membrane potential changes may be superimposed by sodium spikes of

variable amplitude (Haag et al. 1997). Wide-field motion in the opposite direction results in hyperpolarizing membrane potential changes (Hausen 1982b). In addition to the ipsilateral input, HSN and HSE receive contralateral motion signals via heterolateral connecting elements that are sensitive to back-to-front motion (Hausen 1976a, 1981, 1982b; Horstmann et al. 2000). Although the overall response properties are well investigated in the HS neurons (Hausen 1982a,b), information about their binocular receptive field organization with respect to the distribution of local preferred directions and motion sensitivities was not known.

Figure 2 shows the binocular response fields of HSN and HSE. According to its dendritic branching pattern, HSN is more sensitive to motion in equatorial to dorsal parts of the ipsilateral visual field. The maximum motion sensitivity of this neuron was found slightly above the eye equator at an azimuth of about 0 – 15° (Fig. 2A) (cf. Hausen 1982b). From this region, the LMSs decrease toward the dorsal, caudal, and contralateral parts of the response field. Within the ventral ipsilateral visual field HSN does not respond to motion. The ipsilateral response field of HSE comprises extended parts of the equatorial visual hemisphere that corresponds to its dendritic arborizations within the medial part of the lobula plate. HSE shows a sensitivity maximum around an azimuth between 0 and 15° at an elevation of about -15° (Fig. 2B) (cf. Hausen 1982b). The motion sensitivity levels off toward the dorsal and ventral visual field. The LPDs deviate from the exact horizontal in most of the HSN and HSE response fields. In the frontal response field, LPDs determined above and below the eye equator are tilted upward and downward, respectively (cf. Hausen 1982b). Deviations in the opposite directions can be found in caudal parts of the response fields. LPDs oriented about horizontally are confined to the equatorial and lateral parts of the response fields (Fig. 2, A and B).

The contralateral input to HSN and HSE has only a small impact on the averaged membrane potential of these neurons (Hausen 1982a). Therefore applying our evaluation procedure (see METHODS) results in relatively small local motion sensitivities. To visualize the LPDs determined on contralateral stimulation in Fig. 2, the length of the arrows within the framed areas were scaled up by a factor of three (HSN) and two (HSE), respectively. In this part of the response fields, both neurons respond preferably to horizontal back-to-front motion along the eye equator. Only in the frontolateral region around an azimuth of -45° within the HSE response field the LPDs are slightly tilted downward. This deviation from the horizontal is most likely caused by the LPD distributions of the heterolateral elements that mediate the sensitivity of HSE to contralateral motion stimuli.

CH neurons

There are two CH neurons in each lobula plate, the VCH and the DCH (V, ventral; D, dorsal) (Eckert and Dvorak 1983; Hausen 1976a, 1984). The somata of the CH neurons are connected via the primary neurite to their respective main arborization in the contralateral part of the brain (see Fig. 3, *inset*) (cf. Hausen 1993). CH neurons pick up inhibitory and excitatory inputs from the contralateral visual field in the lateral protocerebrum (see Fig. 3, *inset*) (cf. Gauck et al. 1997; Hausen 1976a, 1984, 1993). In addition, the CH neurons re-

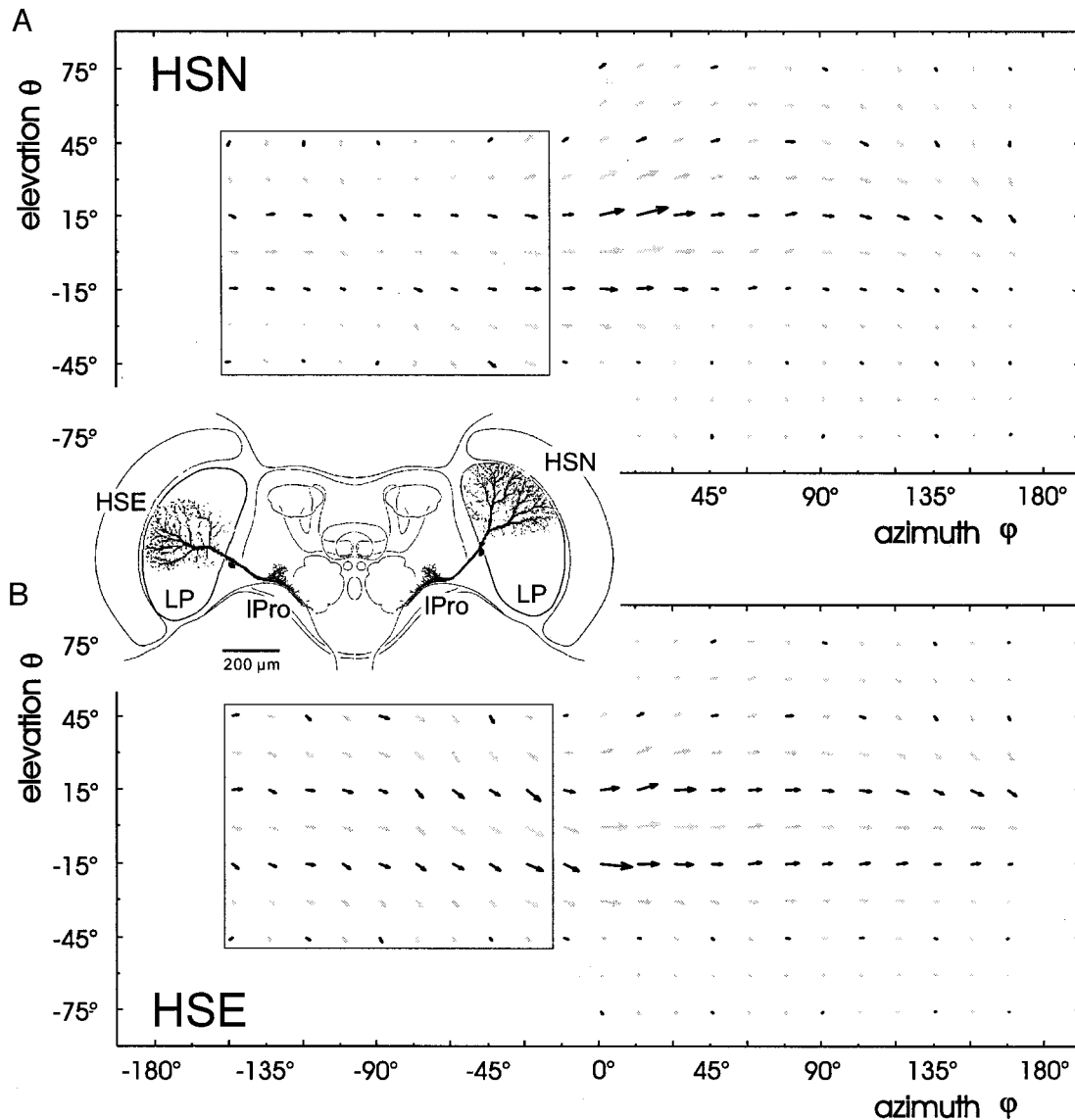


FIG. 2. Mean binocular response field of horizontal systems north (HSN; A, $n = 2$) and east (HSE; B, $n = 3$) and neuronal reconstructions (*inset*) (combined from Hausen 1982a, 1993). To better show the individual arborization pattern of HSN and HSE, which partly overlap, the dendrites of the HSE are plotted within the contour line of the left lobula plate (LP). The response fields shown in A and B belong to neurons both receiving their retinotopic input within the right LP. The LPDs and LMSs are plotted as arrows within a Mercator map of the visual field. Black arrows indicate measured data; gray arrows were obtained by interpolation. An azimuth and elevation of 0° corresponds to the point directly in front, an azimuth of $\pm 180^\circ$ and an elevation of 0° indicates the point directly behind the animal. Positive and negative elevations describe the top and bottom part of the hemisphere, respectively. To emphasize the relatively small responses to contralateral motion stimuli, the arrow length within the framed areas of the response fields are scaled up by a factor of 3 (HSN) and 2 (HSE), respectively. LPro, lateral protocerebrum.

ceive retinotopic input to their extended arborizations within the lobula plate (Dürr and Egelhaaf 1999; Egelhaaf et al. 1993). CH neurons whose main arborization is located within the right half of the brain are predominantly excited by front-to-back motion in front of the right eye and by back-to-front motion within the contralateral visual hemisphere (Egelhaaf et al. 1993; Hausen 1981). VCH was identified to be a wide-field inhibitor responsible for the small-field tuning of the figure detection neuron FD1 (Egelhaaf 1985; Warzecha et al. 1993).

The response fields of DCH and VCH extend over almost the entire visual field (Fig. 3, A and B). Compared to the HS neurons, CH neurons respond more strongly to contralateral motion stimuli. The right part of the DCH response field shows

a broad sensitivity distribution with high LMSs slightly above the eye equator in the frontal and caudal visual field (Fig. 3A). The DCH responds predominantly to horizontal motion along the equatorial regions of the left eye up to the lateral part of the right eye. Only in the caudal parts of the right visual hemisphere do the LPDs tilt downward. The sensitivity maximum of VCH lies in the frontal visual field slightly below the equator (Fig. 3B). Unlike in DCH, the sensitivity decreases more steeply in all directions. A high sensitivity is maintained along the equatorial region within the right visual field where VCH is excited by horizontal front-to-back-motion. In the frontal to lateral region of the left visual field, the LPDs are tilted downward. Toward the caudolateral part along the left

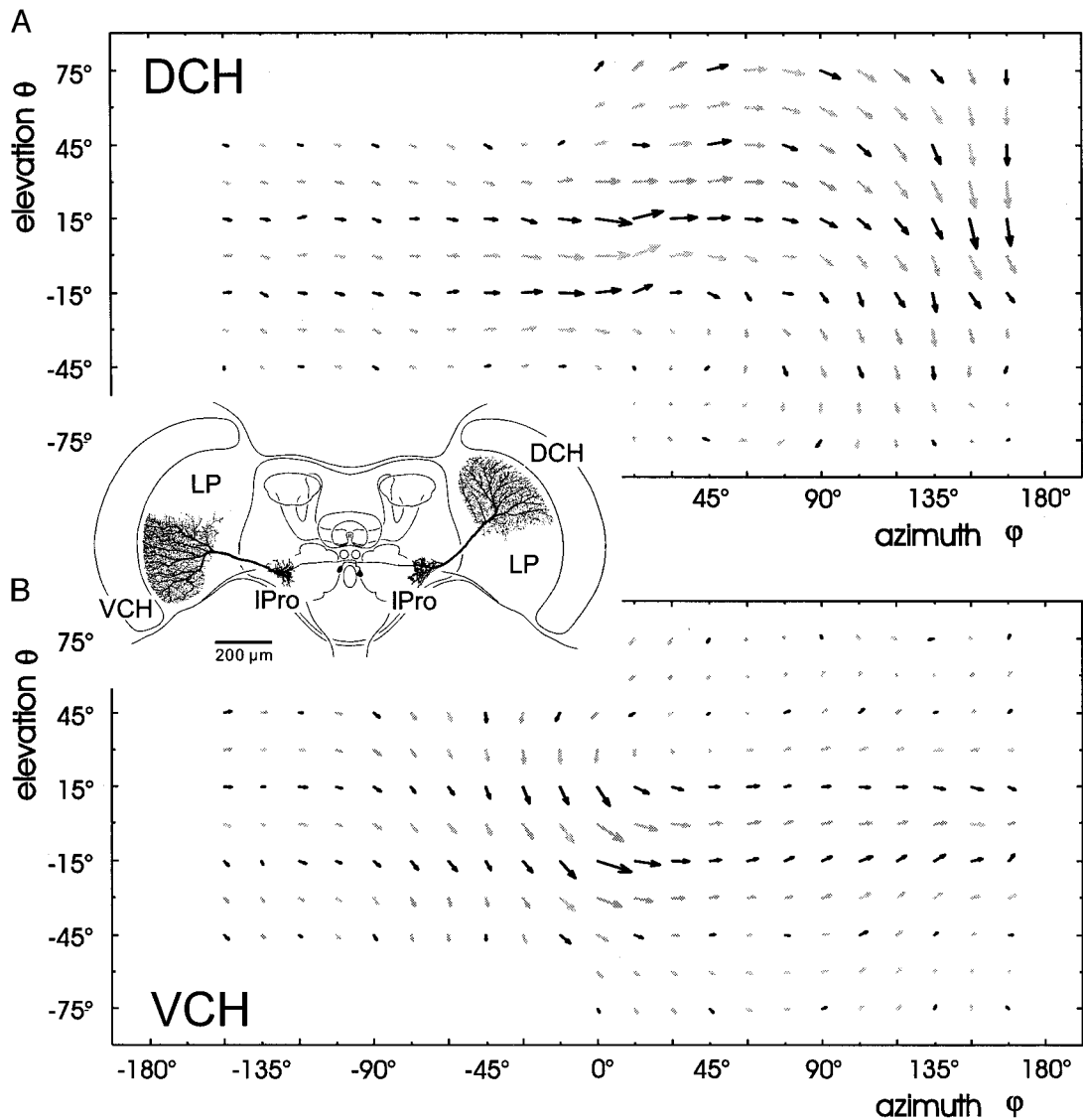


FIG. 3. Mean binocular response fields of DCH (A, $n = 3$) and VCH (B, $n = 2$) and neuronal reconstructions (*inset*) (modified from Hausen 1993). As in Fig. 2, for clarity, the major dendritic field of VCH was plotted to the left half of the brain although the mean response field shown was derived from individuals that receive retinotopic input from the right eye. Both neurons have a large response fields. In the caudal equatorial part of the DCH response field, the orientation of the LPDs deviate from the horizontal. Similar deviations can be found within the VCH response field around the equator of the frontal to lateral part of the left visual hemisphere.

eye equator, the LPDs continuously change their orientation and finally become aligned almost horizontally.

Heterolateral elements H1, H2, and V1

H1 receives retinotopic input and conveys action potentials to its output regions in the contralateral lobula plate (Hausen 1976b). The dendritic arborization of H1 covers almost the whole lobula plate (see Fig. 4, *inset*) (cf. Hausen 1976b, 1993). Its output region covers wide parts of the contralateral lobula plate where it is thought to form input to HSE, DCH, and VCH (see Fig. 4, *inset*) (cf. Hausen 1976b; Horstmann et al. 2000). H2 has a similar input organization but propagates its spikes to the contralateral lateral protocerebrum where it is thought to contact HSN and HSE as well as the CH neurons (see Fig. 4, *inset*) (cf. Hausen 1981). Its dendrites are less extended than

those of H1. V1 picks up information in the terminal region of part of the VS neurons of the ipsilateral lobula plate and propagates spikes to its own output arborizations in the contralateral lobula (see Fig. 4, *inset*) (cf. Hausen 1984, 1993). To allow for an easier comparison with the input organization of their putative target neurons, the response fields of the heterolateral elements of the right part of the brain are plotted as if they were obtained from their respective counterparts originating in the left half of the brain.

The H1 response field comprises almost the entire ipsilateral visual hemisphere. Due to the region of binocular overlap, it includes a small portion of the contralateral hemisphere (Fig. 4A). H1 responds preferentially to horizontal back-to-front motion (cf. Hausen 1976b). Its sensitivity maximum is found in the equatorial region at an azimuth of about -15° . The sensitivity slightly decreases from frontal to caudal. In the most

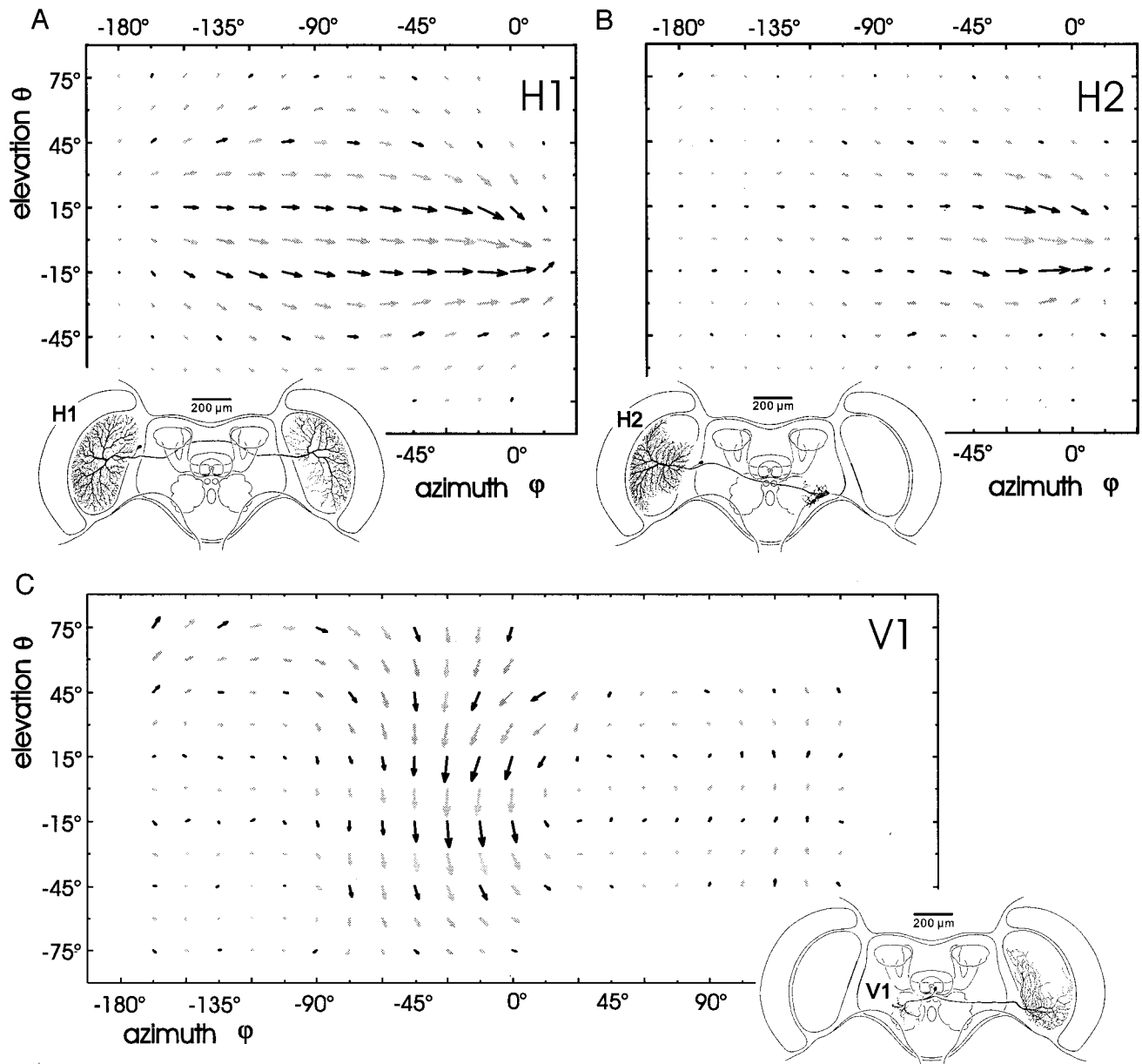


FIG. 4. Mean response fields of H1 (A, $n = 6$), H2 (B, $n = 1$), and V1 (C, $n = 2$) and neuronal reconstructions (*inset*) (modified from Hausen 1993). The response fields are plotted as recorded from neurons that receive their retinotopic input in the left visual hemisphere. Correspondingly, the anatomy is shown for H1, H2, and V1 of the left lobula plate. Note that the distributions of LPDs within the H1 and H2 response fields are very similar, but the sensitivity distribution of the H1 neuron is much broader compared with H2. Both H1 and H2 may be excited by rotations of the animal around about the vertical body axis to the left and inhibited during forward translation. Parts of the V1 response field show similarities with an optic flow field generated during rotation of the animal around the transverse body axis.

dorsal and ventral parts of the visual field, H1 is insensitive to motion. In the frontal part of the response field, the LPDs above the equator are tilted downward, whereas the LPDs below the equator point slightly upward. The LPD distribution of the H2 is very similar to that of H1 (cf. Fig. 4, A and B). Moreover, H2 is also sensitive to horizontal back-to-front motion. The H2 response field, however, is less extended because in the caudal direction, its motion sensitivity decreases more rapidly than that of H1. The V1 response field comprises wide parts of the visual field (Fig. 4C). Its maximum sensitivity can be found in the azimuth range of 0–30° around the eye's equator. The LPDs of V1 continuously change from vertical

downward in the frontolateral, to horizontal in the dorsolateral, to obliquely vertical upward in the dorsocaudal visual field. At an azimuth of about 120°, V1 is slightly sensitive to vertical upward motion; this indicates that VS neurons converging on V1 have—at least partly—binocular receptive fields (Hengstenberg, personal observation).

Preferred self-motion parameters of HS and CH neurons

Given the binocular response field organization of HS and CH neurons, what rotatory and translatory self-motions can be particularly well analyzed by these tangential neurons? To

provide an answer to this question, we first determined the optimal combination of self-rotation and -translation, resulting in an optic flow field the local velocity vector distribution of which most closely approximate the neuronal response field. At any given location within the optic flow field each velocity vector is defined by the vectors \mathbf{R} and \mathbf{T} , describing the rotatory and translatory component of self-motion, respectively. To determine \mathbf{R} and \mathbf{T} , we interpreted the response fields as “noisy” optic flow fields and applied an iterative least-square algorithm developed by Koenderink and van Doorn (1987) (KvD). Since the KvD is based on averaged sums of local velocity vectors, we need to make two assumptions. First, the local motion signals of the elementary movement detectors (EMDs) converging on the tangential neurons are proportional to the velocity of the local retinal image shifts, and second, the tangential neurons linearly integrate the local motion signals. The EMD responses, however, represent the velocity of a given motion stimulus only within a limited dynamic range. In addition, EMD responses depend on the spatial frequency content and the contrast of the stimulus pattern (review: Egelhaaf and Borst 1993). Furthermore tangential neurons linearly integrate only a small number of local motion signals, but for an increasing number of activated local inputs, they show a kind of saturation characteristic (Borst et al. 1995; Hausen 1982b; review: Egelhaaf and Warzecha 1999). Nevertheless, we used the KvD to obtain a first approximation of the neuron’s preferred self-rotation and -translation. For the same reason, we assumed in our calculation an isotropic distribution of distances between the eyes and the visual structures of the surroundings. The latter assumption allowed us to determine not only the direction of \mathbf{R} and \mathbf{T} but also to assess their relative magnitude. The results for the HS and CH neurons are listed in Table 1.

The preferred rotation axes of HSN and HSE are oriented about vertically, resulting in the high specificity for sensing the flow components induced during yaw-rotations of the animal to the left. The preferred translations of the HS neurons slightly deviate from the straight-ahead direction. They point to the frontolateral left visual hemisphere slightly above the horizontal. Thus HS neurons appear to be specialized to sense yaw rotation, which may be superimposed by a translations in the horizontal plane, slightly to the left.

The preferred rotation axes of the CH neurons deviate by about 35° from the vertical body axis of the fly. In case of DCH, the axis is tilted toward the caudolateral aspect of the left visual hemisphere, whereas the preferred rotation axis of VCH is tilted toward the frontolateral part of the right visual hemi-

sphere. Both CH neurons prefer a translation to the dorso-equatorial region of the frontolateral left visual hemisphere. From their preferred self-motion parameters, CH neurons are particularly sensitive to upward banked turns of the fly to the left. For both the HS and the CH neurons, the relative magnitude of \mathbf{R} was on average about 2–2.5 times higher than the magnitude of \mathbf{T} (cf. Table 1). This indicates that the respective distributions of LPDs within the response fields of these neurons more closely approximate optic flow fields induced during particular self-rotations of the fly than during translations.

Significance of binocular input for optic flow processing

To what degree does binocular input increase the neurons’ specificity to particular self-movements? To answer this question, we estimate the neurons’ responses to an optic flow field induced by their preferred combination of self-rotation and -translation ($\mathbf{FF}_{(\mathbf{R}+\mathbf{T})}$) as well as for optic flow fields induced by self-rotation ($\mathbf{FF}_{(\mathbf{R})}$) and self-translation ($\mathbf{FF}_{(\mathbf{T})}$) alone. The estimations were carried out under two conditions: First, the neurons integrate monocular local motion information only, which is basically motion information sampled by retinotopically arranged movement detectors within the right visual hemisphere including the first meridian of the left visual hemisphere ($-15^\circ \leq \varphi \leq 165^\circ$). Second, the neurons integrate binocular local motion information; the left and right visual hemispheres are considered ($-150^\circ \leq \varphi \leq 165^\circ$). In both cases, the preferred self-motions for each neuron, i.e., \mathbf{R} , \mathbf{T} , and their respective relative magnitudes, were taken from Table 1.

To estimate the neurons’ responses to the optic flow fields $\mathbf{FF}_{(\mathbf{R}+\mathbf{T})}$, $\mathbf{FF}_{(\mathbf{R})}$, and $\mathbf{FF}_{(\mathbf{T})}$, we calculated, as a first approximation, the geometrical projection of the respective optic flow fields into the response fields \mathbf{RF} according to

$$SF_{(\mathbf{R}+\mathbf{T})} = (\mathbf{FF}_{(\mathbf{R}+\mathbf{T})} \cdot \mathbf{RF})$$

$$SF_{(\mathbf{R})} = (\mathbf{FF}_{(\mathbf{R})} \cdot \mathbf{RF})$$

$$SF_{(\mathbf{T})} = (\mathbf{FF}_{(\mathbf{T})} \cdot \mathbf{RF})$$

The geometrical projection (dot product) of the local motion vectors into the LPDs closely approximates the cosine-shaped directional tuning characteristic of the tangential neurons (cf. Fig. 1C) (e.g., Hausen 1982b). The projections were calculated only at response field positions where the local response properties of the neuron were experimentally obtained. The procedure results for each neuron in three scalar fields, $SF_{(\mathbf{R}+\mathbf{T})}$, $SF_{(\mathbf{R})}$, and $SF_{(\mathbf{T})}$, which represents the neuron’s local response

TABLE 1. Estimated preferred self-motion vectors of HSN, HSE, DCH, and VCH

| | Preferred Rotation \mathbf{R} | | | Preferred Translation \mathbf{T} | | |
|-----|---------------------------------|-------------------------------|------------------------------------|------------------------------------|-------------------------------|------------------------------------|
| | Azimuth φ , $^\circ$ | Elevation θ , $^\circ$ | Relative Magnitude of \mathbf{R} | Azimuth φ , $^\circ$ | Elevation θ , $^\circ$ | Relative Magnitude of \mathbf{T} |
| HSN | -86 | 79 | 0.20 | -38 | 12 | 0.11 |
| HSE | -28 | 82 | 0.24 | -43 | 23 | 0.10 |
| DCH | -117 | 54 | 0.34 | -55 | 51 | 0.18 |
| VCH | 44 | 56 | 0.30 | -53 | 65 | 0.10 |

Estimated preferred self-motion vectors \mathbf{R} and \mathbf{T} of horizontal system north and east (HSN and HSE), DCH, and VCH. To estimate the preferred self-motions, we applied an iterative least-square algorithm developed by Koenderink and van Doorn (1987). The algorithm computes the self-rotation and -translation vectors \mathbf{R} and \mathbf{T} used to calculate optic flow fields that most closely approximate the distributions of local preferred directions (LPDs) and local motion sensitivities (LMSs) within the neuronal response fields. The orientation of the preferred axis of rotation and the preferred direction of translation is indicated by the angles of azimuth φ and elevation θ ; the magnitude of the respective parameters is given in relative units (for further explanation, see text).

TABLE 2. *Estimated monocular and binocular responses*

| | Estimated Responses to $\mathbf{FF}_{(R+T)}$, $\mathbf{FF}_{(R)}$, and $\mathbf{FF}_{(T)}$, rel. units | | | | | | | | |
|-----|---|-----------|-----------|-------------|-----------|-----------|---|------------------|------------------|
| | Monocular | | | Binocular | | | Response Increments for Binocular Input | | |
| | $r_{(R+T)}$ | $r_{(R)}$ | $r_{(T)}$ | $r_{(R+T)}$ | $r_{(R)}$ | $r_{(T)}$ | $\Delta r_{(R+T)}$ | $\Delta r_{(R)}$ | $\Delta r_{(T)}$ |
| HSN | 13.1 | 10.3 | 6.9 | 14.1 | 11.6 | 6.9 | 1.0 | 1.3 | 0.0 |
| HSE | 12.5 | 10.3 | 6.4 | 14.8 | 13.2 | 6.4 | 2.3 | 2.9 | 0.0 |
| DCH | 18.6 | 15.1 | 10.5 | 21.7 | 18.9 | 9.8 | 3.1 | 3.8 | -0.7 |
| VCH | 13.1 | 10.6 | 3.4 | 17.1 | 15.7 | 6.0 | 4.0 | 4.3 | 2.6 |

Estimated monocular and binocular responses of HSN, HSE, DCH, and VCH to optic flow fields induced by the combination of the preferred self-rotation and translation ($\mathbf{FF}_{(R+T)}$), the preferred self-rotation ($\mathbf{FF}_{(R)}$), and the preferred self-translation ($\mathbf{FF}_{(T)}$). The preferred self-motion parameters (Table 1) were used to calculate optic flow fields that were projected into the respective neuronal response field. The resulting local projections were integrated within the monocular part and the entire binocular response field; the respective responses are given by $r_{(R+T)}$, $r_{(R)}$, and $r_{(T)}$. To assess the effect of binocular contributions to the estimated response, we calculated the respective response increments $\Delta r_{(R+T)}$, $\Delta r_{(R)}$, and $\Delta r_{(T)}$. Note that in all cases, $\Delta r_{(R)}$ is higher than $\Delta r_{(R+T)}$ or $\Delta r_{(T)}$.

contributions to optic flow fields $\mathbf{FF}_{(R+T)}$, $\mathbf{FF}_{(R+T)}$, and $\mathbf{FF}_{(R+T)}$, respectively. To obtain an overall measure of the sensitivity of the neurons to the different optic flow fields, we calculated the linear sum of the local response contributions $SF_{(R+T)}(\varphi, \theta)$, $SF_{(R)}(\varphi, \theta)$, and $SF_{(T)}(\varphi, \theta)$

$$r_{(R+T)} = \sum SF_{(R+T)}(\varphi, \theta)/w(\theta)$$

$$r_{(R)} = \sum SF_{(R)}(\varphi, \theta)/w(\theta)$$

$$r_{(T)} = \sum SF_{(T)}(\varphi, \theta)/w(\theta)$$

where the local response contributions were weighted by a factor $1/w(\theta)$. To avoid any overrepresentation of the local response contributions, the factor $1/w(\theta)$ compensates for different degrees of overlap of the respectively stimulated areas during the experiments to determine the LPDs and LMSs within the spherical visual field. In addition, to keep for each neuron the responses to the different optic flow fields comparable, the absolute sums of local velocity vectors within the flow fields $\mathbf{FF}_{(R+T)}$, $\mathbf{FF}_{(R)}$, and $\mathbf{FF}_{(T)}$ were the same. Since the HS neurons receive no inhibitory input from the contralateral visual hemisphere, their binocular response was only affected when the sum of contralateral projections was greater than 0. In Table 2, the resulting values for $r_{(R+T)}$, $r_{(R)}$, and $r_{(T)}$ are listed that indicate the estimated response of the HS and CH neurons to monocular and binocular optic flow $\mathbf{FF}_{(R+T)}$, $\mathbf{FF}_{(R+T)}$, and $\mathbf{FF}_{(R+T)}$. For all neurons and for monocular as well as binocular contributions, the strongest estimated responses were found for the combination of self-rotation and -translation, closely followed by the estimated responses to rotation alone. The weakest responses were always found for the self-translation. To assess the impact of binocular integration on the neurons' specificity to particular self-movements, we calculated the response increments $\Delta r_{(R+T)}$, $\Delta r_{(R)}$, and $\Delta r_{(T)}$, between the monocular and binocular responses to the three different flow fields (see Table 2).

The response increments $\Delta r_{(T)}$ on binocular input has inconsistent effects on the estimated responses to the preferred translation; it is either zero (HSN, HSE), increases (VCH), or slightly decreases (DCH). The response increments are positive for both the combination of preferred rotation and translation ($\Delta r_{(R+T)}$) and for the preferred rotation ($\Delta r_{(R)}$; see Table 2). For all neurons, however, the response increment $\Delta r_{(R)}$ is higher than $\Delta r_{(R+T)}$ (see Table 2). Thus HS and CH neurons seem to be adapted to indicate the rotatory self-motion component from the flies momentary self-movement.

DISCUSSION

The binocular input organization of fly HS and CH neurons was determined from measurements of the local preferred directions and motion sensitivities within their receptive fields and of their potential contralateral input elements (H1, H2, and V1). Based on the local response properties, we estimated the significance of binocular inputs for the specificity of the neurons for their preferred self-movements.

Experimental evidence for the identity of heterolateral elements transmitting motion information to the HS and CH neurons

The origin of the contralateral input to the HS and CH neurons was established by combined extra- and intracellular double recordings (Haag 1994; Hausen 1976a; Horstmann 2000). HSN was shown to receive contralateral input from H2 in its terminal region (Haag 1994). Since only one class of excitatory postsynaptic potentials (EPSPs) has been noticed in the HSN, an additional excitatory input mediated by another heterolateral element is unlikely. Although the time-averaged responses of HSN to local stimulation in the contralateral visual field are weak, the LPDs determined in the frontolateral part of the contralateral response field are compatible with the LPDs found in the corresponding region of the H2 response field (cf. Figs. 2A and 4B). The tentative binocular input organization of HSN is schematized in Fig. 5A.

In accordance with earlier evidences obtained by Hausen (1981), recent experiments have shown HSE to be postsynaptic to both H1 and H2 (Horstmann et al. 2000). In all double recordings, two classes of EPSPs could be assigned either to H1 or H2 spikes, and it seems unlikely that HSE receives additional contralateral input from a third element (Horstmann et al. 2000). Because we could record sizable responses to local contralateral stimulation, we can compare the contralateral response field of HSE with the H1 and H2 response fields (cf. Figs. 2B and 4, A and B). Although there is a small tendency of the LPDs within the contralateral HSE response field to point downward, the general trend is directed roughly horizontally from back to front. Despite the minor discrepancies in the frontolateral region below the eye equator, H1 and H2 seem to mainly contribute to the organization of the HSE response field (cf. Figs. 2B and 4, A and B). The wiring that most likely accounts for the observed binocular input organization of HSE is illustrated in Fig. 5B.

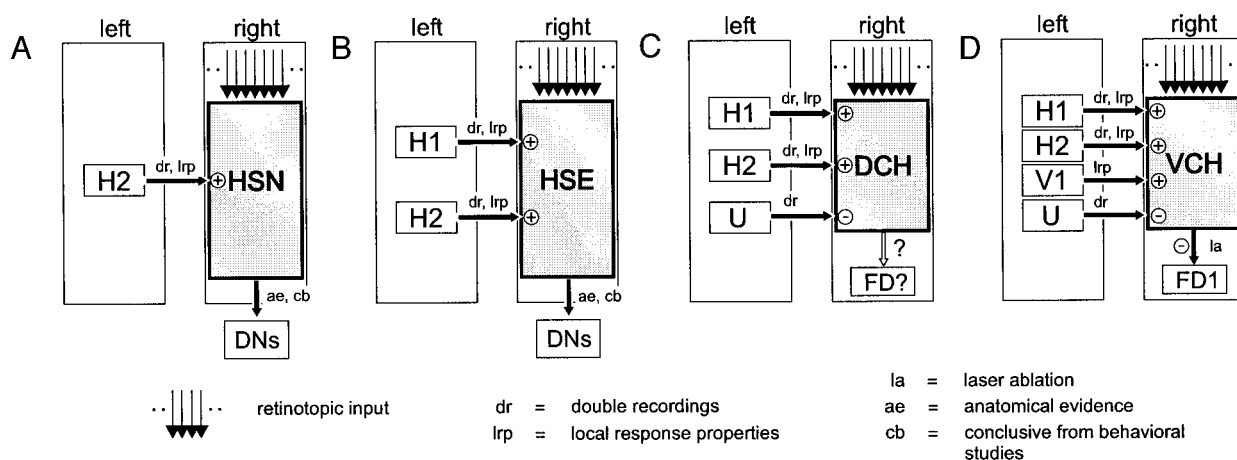


FIG. 5. Schematized binocular input organization of HSN, and HSE and the CH neurons as derived from different lines of evidence. Each circuit refers to the individual HS (A and B) and CH neurons (C and D) receiving their retinotopic input in the right lobula plate. The neurons receive input from heterolateral tangential neurons located in the left lobula plate. Thin vertical arrows indicate the retinotopic input. Thick arrows denote connections suggested by different lines of evidence indicated in the *bottom right* of the figure. + and -, excitatory and inhibitory inputs, respectively. In C and D, the connection between the hitherto unidentified element U is based on correlating U spikes with inhibitory postsynaptic potentials induced in DCH and VCH. Note that the connection of DCH to any figure detection neuron (FD) is hypothetical at this point. More subtle interactions that have been shown to exist, for instance, between the 2 heterolateral H1 neurons (MaCann and Forster 1971), were omitted for clarity. DN, descending neurons.

DCH was shown to receive contralateral input from H1 and H2 and, in addition, from an inhibitory wide-field neuron (element U) that has not yet been anatomically identified (Hausen 1976a). A comparison of the respective response fields supports this conclusion (cf. Figs. 3A and 4, A and B). The influence of element U that is sensitive to horizontal front-to-back motion in the contralateral visual field cannot be judged from the response field. However, because DCH generates inhibitory postsynaptic potentials (IPSPs) when stimulated along the preferred direction of element U, the local motion sensitivity of DCH to contralateral back-to-front motion may be slightly enhanced. A schematic of the DCH input organization is shown in Fig. 5C.

VCH was thought to receive its contralateral motion sensitivity from H1 as well as from H2, although unambiguous double recording experiments are still lacking that might prove this notion. A comparison of the contralateral VCH response field with the H1 and H2 response fields supports this hypothesis only partly. In the frontolateral region of the contralateral visual field, the predominant LPDs point downward instead of being horizontally aligned. The contralateral distribution is more reminiscent of a blend of inputs including H1 and H2 signals but also of an element sensitive to downward motion in the frontolateral visual field. One candidate neuron that may supply the sensitivity to vertical downward motion is V1 (cf. Fig. 4C). In Fig. 5D, the hypothetical binocular input organization of this neuron is illustrated.

Functional significance of extended receptive fields and the binocular input organization of HS and CH neurons for estimating self-motion from optic flow

From a theoretical point of view, improving the performance in estimating self-motion parameters—like the rotation vector \mathbf{R} and the direction of translation \mathbf{T} —from the current optic flow can be achieved by two strategies: the first one concerns the receptive field size and the number of sampling points. By

applying a modified least-square algorithm (Koenderink and van Doorn 1987), numerical simulations showed that self-motion parameters can be reliably estimated from noisy optic flow fields if local motion vectors were analyzed at about 100 sampling points homogeneously distributed within about one visual hemisphere (Dahmen et al. 2000). Indeed, visual interneurons sensitive to optic flow have frequently very large receptive fields (see INTRODUCTION). The second strategy to gain reliable information about the self-motion is to extend the visual field in a way as to include both visual hemispheres. For instance, if a rotation around the vertical axis is to be detected, it is an eminent advantage to analyze motion at positions that are 180° apart on a connecting meridian (Dahmen et al. 1997, 2000). In case of rotation, the two velocity vectors point in opposite directions, whereas during translation, they point in the same direction. Thus a neuron integrating the signals of EMDs whose preferred directions point front-to-back in the lateral right visual hemisphere and back-to-front in the lateral left visual hemisphere can be expected to respond stronger to rotation than to translation. The local rotation responses are added up by the neuron, whereas if the sensitivity is about equal within the two visual hemispheres, the local translation responses cancel out each other.

The receptive field organization of DCH, VCH, HSN, and HSE are well suited for the task of self-motion estimation. These neurons receive signals from thousands of local motion detectors together sensing visual motion within almost the entire visual field. Such a dense sampling may partly compensate for uncertainties inherent to local motion analysis due to, for instance, neuronal noise and the pattern dependence of elementary motion detection. Furthermore densely sampling local motion information has been discussed as an adaptation to cope with sparse distributions of contrasts in some natural scenes (Dahmen et al. 2000). Most important, however, is the fact that HSN and HSE and the CH neurons process binocular

motion information at opposite positions within the visual field.

The sensitivity of HS and CH neurons, in particular to their preferred self-rotation, is increased by taking into account motion within the visual field of both eyes. This is reflected by the result that the response increment $\Delta r_{(R)}$ is in all cases higher than the response increments $\Delta r_{(R+T)}$ and $\Delta r_{(T)}$, respectively. Recent experiments on HSE suggest that the signal structure of this neuron may play a decisive role in encoding self-motion. Response transients, such as spikes and large-amplitude EPSPs, seem to be more specific indicators of self-rotations than the mean membrane potential (Horstmann et al. 2000). Since we time-averaged the responses of the HS neurons, we did not explicitly consider the transient membrane potential fluctuations. Therefore our calculations most likely underestimate the binocular response of HSE to its preferred rotation and the resulting response increment $\Delta r_{(R)}$.

It should be emphasized, however, that the way we estimated the tangential neurons' responses to optic flow fields induced by particular self-motions need to be considered only a first approximation. Beside the simplifications we outlined in RESULTS, we mentioned in the INTRODUCTION that the magnitude of translatory optic flow depends not only on the animal's speed but also on its distance to environmental objects. In our calculations, we assumed the same distances in all directions of the visual field, what is certainly a surrounding the fly will never encounter in nature. In this context, it is important to note that the results obtained under the described assumptions are relatively stable against changes of the distance distribution. For instance, introducing closer distances of the fly to its surroundings in the ventral visual field than in the dorsal visual field (cf. Franz and Krapp 2000), leads to greater differences between the binocular response increments to the preferred rotation and translation, $\Delta r_{(R)}$ and $\Delta r_{(T)}$, respectively. In electrophysiological experiments, we are currently investigating to what extent predictions on the specificity of HS and CH neurons to particular self-rotations that were based on local motion measurements hold true for the neurons' responses on visual wide field stimulation.

With respect to the magnitude of the nonretinotopic input imparting the neurons with binocular vision, we found that the response increment $\Delta r_{(R)}$ to the rotatory optic flow in HS neurons was, on average, only about half as high than in CH neurons (cf. Table 2). With our stimulus procedure, we measured only very small response amplitudes under contralateral stimulation (cf. Fig. 2). This is in accordance with a study by Hausen (1982b) where he reported only a subtle increase of the averaged membrane potential in HSN and HSE on binocular compared with monocular stimulation. He simulated rotational optic flow by back-to-front motion in the frontolateral area of the contralateral and front-to-back motion in the corresponding part of the ipsilateral visual hemisphere. In similar experiments on CH neurons, however, the response to binocular motion was shown to be almost twice as large compared with the response to ipsilateral stimulation alone (Egelhaaf et al. 1993). These findings are in good accordance with our result estimating higher response increments for the preferred rotation $\Delta r_{(R)}$ in CH neurons than in HS neurons.

In summary, the detailed investigation of the local response properties supports the idea that HSN and HSE may be well suited to encode information about self-rotations around the

vertical body axis (about yaw-rotation), which may be superimposed by a translation in the horizontal plane to the left. Since the HS neurons are output elements of the visual system, signals originating from both halves of the visual system could further interact in different ways at subsequent processing stages to lead to more specific representations of different types of self-motion. This information could then be utilized for solving a variety of tasks in flight steering, walking, and gaze stabilization. Such an elaboration of the specificity for optic flow is not possible for the CH cells that are intrinsic elements of the third visual neuropile and seem to indicate banked turns of the animal. Because of their extended binocular response field organization, CH cells are ideally suited wide-field inhibitors, for instance, in the context of figure-ground discrimination (Egelhaaf 1985).

The authors are grateful to K. Hausen for kindly supplying the reconstructions of the tangential neurons and for critically reading and commenting on the manuscript. We also thank R. Kern, R. Kurtz, and A.-K. Warzecha for critically reading and discussing the manuscript. In addition, we thank two anonymous referees for constructive criticism and language corrections that helped to improve the manuscript.

This work was supported by the Max-Planck Gesellschaft and the Deutsche Forschungsgemeinschaft.

REFERENCES

- BATSCHLET E. *Circular Statistics in Biology*. London: Academic, 1981.
- BAUSENWEIN B, WOLF R, AND HEISENBERG M. Genetic dissection of optomotor behavior in *Drosophila melanogaster*. Studies on wild-type and the mutant optomotor-blind. *J Neurogenet* 3: 87–109, 1986.
- BORST A AND EGELHAAF M. Principles of visual motion detection. *Trends Neurosci* 12: 297–306, 1989.
- BORST A, EGELHAAF M, AND HAAG J. Mechanisms of dendritic integration underlying gain control in fly motion sensitive interneurons. *J Comput Neurosci* 2: 5–18, 1995.
- DAHMEN H, FRANZ MO, AND KRAPP HG. Extracting egomotion from optic flow: limits of accuracy and neuronal matched filters. In: *Processing Visual Motion in the Real World—A Survey of Computational, Neuronal, and Ecological Constraints*, edited by Zanker JM and Zeil J. Berlin, Germany: Springer, 2001, p. 143–168.
- DAHMEN H, WÜST RW, AND ZEIL J. Extracting egomotion parameters from optic flow: principal limits for animals and machines. In: *From Living Eyes to Seeing Machines*, edited by Srinivansan MV and Venkatesh S. Oxford, UK: Oxford Univ. Press, 1997, p. 174–198.
- DÜRR V AND EGELHAAF M. In vivo calcium accumulation in presynaptic and postsynaptic dendrites of visual interneurons. *J Neurophysiol* 82: 3327–3338, 1999.
- DVORAK DR, BISHOP LG, AND ECKERT HE. On the identification of movement detectors in the fly optic lobe. *J Comp Physiol* 100: 5–23, 1975.
- ECKERT H AND DVORAK DR. The centrifugal horizontal cells in the lobula plate of the blowfly, *Phaenicia sericata*. *J Insect Physiol* 29: 547–560, 1983.
- EGELHAAF M. On the neuronal basis of figure-ground discrimination by relative motion in the visual system of the fly. II. Figure-detection cells, a new class of visual interneurons. *Biol Cybern* 52: 195–209, 1985.
- EGELHAAF M AND BORST A. Movement detection in arthropods. In: *Visual Motion and its Role in the Stabilization of Gaze*, edited by Miles FA and Wallman J. Amsterdam: Elsevier, 1993, p. 53–77.
- EGELHAAF M, BORST A, WARZECHA A-K, FLECHS S, AND WILDEMANN A. Neuronal circuit tuning fly visual neurons to motion of small objects. II. Input organization of inhibitory circuit elements revealed by electrophysiological and optical recording techniques. *J Neurophysiol* 69: 340–351, 1993.
- EGELHAAF M AND WARZECHA A-K. Encoding of motion in real time by the fly visual system. *Curr Opin Neurobiol* 9: 454–450, 1999.
- FRANCESCHINI N. Sampling of visual environment by the compound eye of the fly: fundamentals and applications. In: *Photoreceptor Optics*, edited by Snyder AW and Menzel R. Berlin, Germany: Springer, 1975, p. 98–125.
- FRANZ MO AND KRAPP HG. Wide-field, motion-sensitive neurons and matched filters for estimating self-motion from optic flow. *Biol Cybern* 83: 185–197, 2000.

- GAUCK V, EGELHAAF M, AND BORST A. Synapse distribution on VCH, an inhibitory, motion-sensitive interneuron in the fly visual system. *J Comp Neurol* 381: 489–499, 1997.
- GEIGER G AND NÄSSEL DR. Visual orientation behaviour of flies after selective laser beam ablation of interneurons. *Nature* 293: 398–399, 1981.
- GIBSON JJ. *The Perception of the Visual World*. Boston, MA: Houghton Mifflin, 1950.
- GÖTZ KG. Bewegungssehen und Flugsteuerung bei der Fliege *Drosophila*. In: *BIONA-Report*, edited by Nachtigall W. Stuttgart, Germany: G. Fischer, 1983, p. 21–34.
- GRONENBERG W AND STRAUSFELD NJ. Descending neurons supplying the neck and flight motor of diptera: physiological and anatomical characteristics. *J Comp Neurol* 302: 973–991, 1990.
- HAAG J. *Aktive und passive Membraneigenschaften bewegungsempfindlicher Interneurone der Schmeissfliege Calliphora erythrocephala* (PhD dissertation). Tübingen, Germany: Universität Tübingen, 1994.
- HAAG J, THEUNISSEN F, AND BORST A. The intrinsic electrophysiological characteristics of fly lobula plate tangential cells. II. Active membrane properties. *J Comput Neurosci* 4: 349–369, 1997.
- HAUSEN K. *Struktur Funktion und Konnektivität bewegungsempfindlicher Interneurone im dritten optischen Neuropil der Schmeissfliege Calliphora erythrocephala* (PhD dissertation). Tübingen, Germany: Universität Tübingen, 1976a.
- HAUSEN K. Functional characterization and anatomical identification of motion sensitive neurons in the lobula plate of the blowfly *Calliphora erythrocephala*. *Z Naturforsch* 31: 629–633, 1976b.
- HAUSEN K. Monocular and binocular computation of motion in the lobula plate of the fly. *Verh Dtsch Zool Ges* 74: 49–70, 1981.
- HAUSEN K. Motion sensitive interneurons in the optomotor system of the fly. I. The horizontal cells: structure and signals. *Biol Cybern* 45: 143–156, 1982a.
- HAUSEN K. Motion sensitive interneurons in the optomotor system of the fly. II. The horizontal cells: receptive field organization and response characteristics. *Biol Cybern* 45: 143–156, 1982b.
- HAUSEN K. The lobula-complex of the fly: structure, function and significance in visual behaviour. In: *Photoreception and Vision in Invertebrates*, edited by Ali MA. New York: Plenum, 1984, p. 523–559.
- HAUSEN K. Decoding of retinal image flow in insects. In: *Visual Motion and its Role in the Stabilization of Gaze*, edited by Miles FA and Wallman J. Amsterdam: Elsevier, 1993, p. 203–235.
- HAUSEN K AND EGELHAAF M. Neural mechanisms of visual course control in insects. In: *Facets of Vision*, edited by Stavenga DG and Hardie RC. Berlin, Germany: Springer, 1989, p. 391–424.
- HAUSEN K AND WEHRHAHN C. Neuronal circuits mediating visual flight control in flies. I. Quantitative comparison of neuronal and behavioral response characteristics. *J Neurosci* 9: 3828–3836, 1989.
- HAUSEN K AND WEHRHAHN C. Neuronal circuits mediating visual flight control in flies. II. Separation of two control systems by microsurgical brain lesions. *J Neurosci* 10: 351–360, 1990.
- HEISENBERG M, WONNEBERGER R, AND WOLF R. Optomotor-blind^{H31}—a *Drosophila* mutant of the lobula plate giant neurons. *J Comp Physiol* 124: 287–296, 1978.
- HENGSTENBERG R. Gain differences of gaze-stabilizing head movements, elicited by wide-field pattern motions, demonstrate in wildtype and mutant *Drosophila*, the importance of HS- and VS-neurons in the third visual neuropil for the control of turning behaviour (Abstract). In: *Nervous Systems and Behaviour. Proceedings of the Fourth International Congress on Neuroethology*, edited by Burrows M, Matheson PL, Newland H, and Schuppe H. Stuttgart, Germany: Thieme, 1995, p. 264.
- HORSTMANN W, EGELHAAF M, AND WARZECHA A-K. Synaptic interactions increase optic flow specificity. *Eur J Neurosci* 12: 2157–2165, 2000.
- IBBOTSON MR. Wide-field motion sensitive neurons tuned to horizontal movement in the honeybee *Apis mellifera*. *J Comp Physiol [A]* 168: 91–102, 1991.
- KERN R. Visual position stabilization in the hummingbirds hawk moth, *Macroglossum stellatarum* L. II. Electrophysiological analysis of neurons sensitive to wide-field image motion. *J Comp Physiol [A]* 182: 239–249, 1998.
- KERN R, NALBACH H-O, AND VARJÚ D. Interactions of local movement detectors enhance the detection of rotation. Optokinetic experiments with the rock crab *Pachygrapsus marmoratus*. *Vis Neurosci* 10: 643–652, 1993.
- KOENDERINK JJ AND VAN DOORN AJ. Facts on optic flow. *Biol Cybern* 56: 247–254, 1987.
- KERN R AND VARJÚ D. Visual position stabilization in the hummingbirds hawk moth, *Macroglossum stellatarum* L. I. Behavioural analysis. *J Comp Physiol [A]* 182: 225–237, 1998.
- KRAPP HG. Neuronal matched filters for optic flow processing in flying insects. *Int Rev Neurobiol* 44: 93–120, 2000.
- KRAPP HG AND HENGSTENBERG R. Estimation of self-motion by optic flow processing in single visual interneurons. *Nature* 384: 463–466, 1996.
- KRAPP HG AND HENGSTENBERG R. A fast procedure to determine local receptive field properties of motion-sensitive visual interneurons. *Vis Res* 37: 225–234, 1997.
- KRAPP HG, HENGSTENBERG B, AND HENGSTENBERG R. Dendritic structure and receptive-field organization of optic flow processing interneurons in the fly. *J Neurophysiol* 79: 1902–1917, 1998.
- LAPPE M (Editor). Neuronal processing of optic flow. In: *International Review of Neurobiology, Vol. 44*. San Diego, CA: Academic, 2000.
- LAPPE M, BREMMER F, AND VAN DEN BERG AV. Perception of self-motion from optic flow. *Trends Cognit Sci* 3: 329–336, 1999.
- LEONARD CS, SIMPSON JJ, AND GRAF W. Spatial organization of visual messages of the rabbit's cerebellar flocculus. I. Topology of inferior olive neurons of the dorsal cap of Kooy. *J Neurophysiol* 60: 2073–2090, 1988.
- MACANN GD AND FORSTER SF. Binocular interactions of motion detection fibers in the optic lobes of flies. *Kybernetik* 8: 193–203, 1971.
- NALBACH H-O AND NALBACH G. Distribution of optokinetic sensitivity over the eye of crabs: its relation to habitat and possible role on flow-field analysis. *J Comp Physiol [A]* 160: 127–135, 1987.
- WARZECHA AK, EGELHAAF M, AND BORST A. Neural circuit tuning fly visual interneurons to motion of small objects. I. Dissection of the circuit by pharmacological and photoinactivation techniques. *J Neurophysiol* 69: 329–339, 1993.
- WATSON DF. *Contouring. A Guide to the Analysis and Display of Spatial Data*. New York: Pergamon, 1994.
- WYLIE DRW AND FROST BJ. Responses of neurons in the nucleus of the basal optic root to translational and rotational flowfields. *J Neurophysiol* 81: 267–276, 1999.